Convergence Properties of Direct Position and Speed Estimation in Synchronous Motor Drives

Matthias Preindl, *IEEE Senior Member*
Department of Electrical Engineering, Columbia University in the City of New York, New York, NY 10027, USA
matthias.preindl@columbia.edu

***Abstract*—This paper analyzes direct position and speed estimation from a control theoretical and numerical standpoint. The paper develops the theory of local identifiability and defines the conditions such that position and speed can be identified uniquely based on a sufficiently accurate guess. Local identifiability typically holds at nonzero machine speeds and zero speeds with any perturbation, e.g. an injected high frequency signal in PWM control or a random switching ripple in direct control (except in isotropic machines). The position and speed is identifiable in more than 98.5% of feasible operation points "instantaneously", and can be extrapolated from past estimates in the remaining cases. Finally, numerical solving strategies are studied and a combination of the Newton and conjugate gradient method is shown to provide suitable estimates within 1-5 solver iterations depending on the required accuracy.**

***Index Terms*—Estimation, Motor Drives, Numerical Stability, Optimization Methods**

I. Introduction

Synchronous motor drives requires an accurate rotor position and speed information for high performance control. Position sensorless estimation schemes have been introduced to remove the cost of a resolver or encoder and improve their reliability by removing a single point of failure. These arguments are especially compelling in mass-produced drive systems, e.g. in hybrid and electric vehicles, when the machine is physically distant from the motor controller, e.g. pumps for underground mining or wind power plants with converter at the tower base, the available space for a motor drive is restricted, e.g. low power drives, or a drive system operates in hazardous or clean environments, where physical contact between stator and rotor is undesired.

Direct position and speed sensorless estimation obtain the position and speed information from an optimization problem. The concept is based on [1], [2] removing any form of filtering, that yields: (i) "instantaneous" estimation by extracting position and speed estimation from the measurements of one sample (two samples if the current derivative is computed from two adjacent samples), (ii) a single scheme for low and high speed position estimation, (iii) compatibility with any perturbation, i.e. any signal injection technique or exploiting the current ripple, for low speed estimation, (iv) compatibility with nonlinear motor models that account for saturation. The concept consists in identifying the position and speed based on a least squares formulation of the dynamic model parametrized with the measurements of one sample. The resulting cost function is nonlinear in the estimates and is solved numerically in real time. This approach with added PLL filtering has been studied experimentally for applications that require highly dynamic torque control, e.g. belt-starter-generator drives that must crank an engine or electric vehicle traction motor drives. It was combined with PWM control, e.g. vector control or convex control set model predictive control (CCS-MPC) [1], which uses a high frequency perturbation for low speed estimation, and direct control, e.g. finite control set model predictive control (FCS-MPC) [2], which uses the inherent random switching ripple for low speed estimation. It can also take magnetic saturation into account [3] and can be applied to induction motor drives [4]. A block diagrams is shown in Fig. 1.

This paper studies the control-theoretical requirements such that position and speed are identifiable based on the measurements of a single sample. The resulting mathematical tools are useful to identify occasional poor estimates, which should be discarded and provide estimation guarantees, despite of the position and speed estimation problem's lack of globally observability [5], [6]. This research focuses on local identifiability, i.e. the requirements that both parameters can be estimated at each sampling instant, based on a sufficiently accurate initial guess. Furthermore, we study the numerical complexity of direct position sensorless estimation.

This paper is organized a follows. The robust identifiability theory is developed in Section II for a generic nonlinear system and applied to synchronous motor drives in Section III and Section IV. The numerical aspects are treated in Section V.

II. Direct Estimation

A. Definition and local parameter identifiability

The concept of direct parameter estimation is described for the nonlinear dynamic system $\dot{x} = f(x, u, z)$, with states $x \in \mathbb{X} \subseteq \mathbb{R}^n$, inputs $u \in \mathbb{U} \subseteq \mathbb{R}^m$, and unknown parameters $z \in \mathbb{Z} \subseteq \mathbb{R}^l$ at time instant t. In sampled systems, the time derivative $\dot{x}$ is typically approximated with the finite difference of two adjacent x. We assume that $f : \mathbb{X} \times \mathbb{U} \times \mathbb{Z} \to \mathbb{R}^n$ is smooth and the sets $\mathbb{X}$, $\mathbb{U}$, and $\mathbb{Z}$ are convex. Direct estimation uses the known states x and inputs u to generate an estimate $\hat{z} = z + \tilde{z}$, where $\tilde{z}$ is the estimation error. The residuals of the dynamic system

$$r(\hat{z}) = f(x, u, \hat{z}) - \dot{x}, \tag{1}$$

act as a qualifier of an estimate $\hat{z}$ in the sense that $r(\hat{z}) = 0$ is a *necessary* condition such that $\hat{z} = z$, i.e. $\tilde{z} = 0$. In other words, $\hat{z} = z$ implies $r(\hat{z}) = 0$ but the reverse is not true in general and additional provisions are necessary. Direct parameter estimation fits the parameters in a nonlinear least squares sense with the optimization problem

$$\hat{z}^\star = \arg\min_{\hat{z} \in \mathscr{D}} c(\hat{z}) = \|r(\hat{z})\|^2 = r(\hat{z})' r(\hat{z}), \tag{2}$$

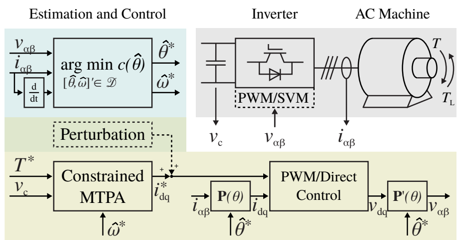

Fig. 1. Direct position and speed estimation for PWM control, e.g. vector control or CCS-MPC, and direct control, e.g. FCS-MPC, with optional high frequency perturbation

with the cost function $c : \mathbb{Z} \to \mathbb{R}$ and search domain $\mathcal{D} \subseteq \mathbb{Z}$. Without loss of generality, we shift the problem in the origin

$$\tilde{r}(\tilde{z}) = r(z + \tilde{z}) = f(x, u, z + \tilde{z}) - \dot{x}, \tag{3}$$

and obtain the modified optimization problem

$$\tilde{z}^{\star} = \arg\min_{\tilde{z}\in\tilde{\mathcal{D}}} \tilde{c}(\tilde{z}) = \|\tilde{r}(\tilde{z})\|^2 = \tilde{r}(\tilde{z})'\tilde{r}(\tilde{z}), \tag{4}$$

with error cost function $\tilde{c}(\cdot) : \mathbb{Z} - \{z\} \to \mathbb{R}$ and search domain $\tilde{\mathcal{D}} = \mathcal{D} - \{z\}$. The error formulation permits studying the solutions of (4) where $\tilde{z}^{\star} = 0$ identifies $\hat{z}^{\star} = z$.

Local identifiability establishes whether the parameters can be identified based on a sufficiently accurate guess $\tilde{z}_g$. The parameters are said to be *locally identifiable* if the minimizer $\tilde{z}^{\star} = 0$ is unique in its immediate neighborhood. This definition requires the origin to be a strict, which holds for smooth functions with strictly convex origin [7].

B. Search domain

Local identifiability requires a strict minimum that is unique in a quasiconvex neighborhood of the origin [7]. Hence, viable search domains are identified introducing the set of *local strict convexity* $\tilde{\mathcal{Z}}$ and the set of *local quasiconvexity* $\tilde{\mathcal{Q}}$

$$\tilde{\mathcal{Z}} = \left\{\tilde{z} \in \mathbb{R}^l \mid \mathcal{H}_{\tilde{c}}(\tilde{z}) \geq 0\right\}, \tag{5a}$$

$$\tilde{\mathcal{Q}} = \left\{\tilde{z} \in \mathbb{R}^l \mid \sum \left(\operatorname{eig}\left[\begin{smallmatrix} 0 & (\nabla\tilde{c}(\tilde{z}))' \\ \nabla\tilde{c}(\tilde{z}) & \mathcal{H}_{\tilde{c}}(\tilde{z}) \end{smallmatrix}\right] < 0\right) \leq 1\right\}. \tag{5b}$$

The function is said to be locally convex iff the Hessian is positive definite and locally quasiconvex iff the bordered Hessian has at most one negative eigenvalue (counting multiplicity) [7]. As observed in Fig. 2, $\tilde{\mathcal{Z}}$ and $\tilde{\mathcal{Q}}$ are nonconvex sets in general. However, any convex subset $\tilde{\mathcal{D}} \subseteq \tilde{\mathcal{Q}}$, $0 \in \tilde{\mathcal{D}}$ is a suitable search domain. Restricting the subset to $\tilde{\mathcal{D}} \subseteq \tilde{\mathcal{Z}}$, $0 \in \tilde{\mathcal{D}}$ tends to have numerical advantages (see Section V). An explicit lower bound for $\tilde{\mathcal{D}}$ can be identified by computing the largest ball inscribed in $\tilde{\mathcal{Q}}$ (or $\tilde{\mathcal{Z}}$). However, the resulting program is np-hard for nonconvex sets [7] and therefore avoided in real-time computation.

C. Convexification of the cost function

Nonlinear identification problems typically require a sufficiently accurate guess $\tilde{z}_g \in \tilde{\mathcal{D}}$ to uniquely identify the $\tilde{z}^{\star}$. However, the convexity properties of the origin depend on the dynamic system and it can be challenging to enforce strict convexity persistently, i.e. at all time. Hence, a term can be added to the cost function that enforces strict convexity of the origin

$$\tilde{z}^{\star} = \arg\min_{\tilde{z}\in\tilde{\mathcal{D}}} \ \tilde{c}(\tilde{z}) + \rho\|\tilde{z} - \tilde{z}_g\|^2. \tag{6}$$

The convexity term adds a quadratic cost centered in $\tilde{z}_g$ (as opposed to the unknown origin) and can therefore shift $\tilde{z}^{\star}$ from the origin towards the guess $\tilde{z}_g$. Hence, the *convexification parameter* $\rho \in \mathbb{R}_{>0}$ should be chosen such that $\tilde{c}(\tilde{z}) \gg \rho\|\tilde{z}\|^2$ for $\tilde{z} \in \mathcal{D}$ to prevent unintended modifications of $\tilde{z}^{\star}$. However, even a small ρ binds the parameters to the guess $\tilde{z}_g$ and prevents these dimensions from arbitrary modification when local identifiability does not hold. Examples of such *bad native operation points* (BNO) are shown in Fig. 2. In a sampled system, $\tilde{z}_g$ is typically chosen as the estimate from the previous time step and therefore typically close to the origin.

III. Synchronous Machine Model

A. The implicit dq model

Any permanent magnet synchronous machine (PMSM), wound-rotor (without damper windings), and reluctance synchronous machine (RSM) is described by the dynamic equation in the dq reference frame [8]

$$\dot{\lambda}_{dq} = -\omega \mathbf{J} \lambda_{dq} + \bar{v}_{dq}, \tag{7}$$

where $\lambda_{dq} \in \mathbb{R}^2$ is the stator flux, $\bar{v}_{dq} = v_{dq} - Ri_{dq} \in \mathbb{R}^2$ is the *compensated* terminal voltage with the resistive voltage drop Ri_{dq}, and $\mathbf{J} = [[0, 1]', [-1, 0]']$ is the 90° rotation matrix. In dq, the stator flux and armature (stator) currents are related by a static map in the dq reference frame [9].

$$\lambda_{dq} = l \circ i_{dq} \approx \mathbf{L} i_{dq} + \psi_r, \tag{8}$$

where $l : \mathbb{R}^2 \to \mathbb{R}^2$ is the nonlinear current-flux map. It links dq current and dq flux globally and is computed through finite element analysis (FEA) or measured experimentally. For control purposes, this relation is typically approximated with an affine map with parameters $\mathbf{L} = \operatorname{diag}[L_d, L_q]$ and $\psi_r = [\psi, 0]'$, where L_d and L_q are the d and q axis inductances and ψ is the rotor flux magnitude. We assume that the affine approximation is a fit with reasonable accuracy, e.g. using optimized parameters [9].

B. The explicit αβ model

The implicit position dependence of the dq models is made explicit transforming (7) and (8) into the static $\alpha\beta$ reference frame using the orthogonal Park transformation $\mathbf{P}(\theta) = [[\cos\theta, -\sin\theta]', [\sin\theta, \cos\theta]']$ with $\bar{v}_{dq} = \mathbf{P}(\theta)\bar{v}_{\alpha\beta}$, $\lambda_{dq} = \mathbf{P}(\theta)\lambda_{\alpha\beta}$, and $i_{dq} = \mathbf{P}(\theta) i_{\alpha\beta}$. The dynamic system (7) becomes $\dot{\lambda}_{\alpha\beta} = \bar{v}_{\alpha\beta}$ [8] and the current-flux map (8) results in

$$\lambda_{\alpha\beta} = \mathbf{P}'(\theta)\mathbf{L}\mathbf{P}(\theta) i_{\alpha\beta} + \mathbf{P}'(\theta)\psi_r. \tag{9}$$

The dynamic model and flux map is put into relationship by deriving the latter with respect of time

$$\dot{\lambda}_{\alpha\beta} = \mathbf{P}'(\theta)\mathbf{L}\mathbf{P}(\theta)\dot{i}_{\alpha\beta} + \tfrac{d}{dt}\left(\mathbf{P}'(\theta)\mathbf{L}\mathbf{P}(\theta)\right) i_{\alpha\beta} + \dot{\mathbf{P}}'(\theta)\psi_r.$$

The term $\mathbf{P}'(\theta)\mathbf{L}\mathbf{P}(\theta)$ is written using the sum $L_\Sigma = (L_d + L_q)/2$ and difference $L_\Delta = (L_d - L_q)/2$ inductance [1]

$$\mathbf{P}'(\theta)\mathbf{L}\mathbf{P}(\theta) = L_\Sigma \mathbf{I} + L_\Delta \bar{\mathbf{P}}(2\theta), \tag{10}$$

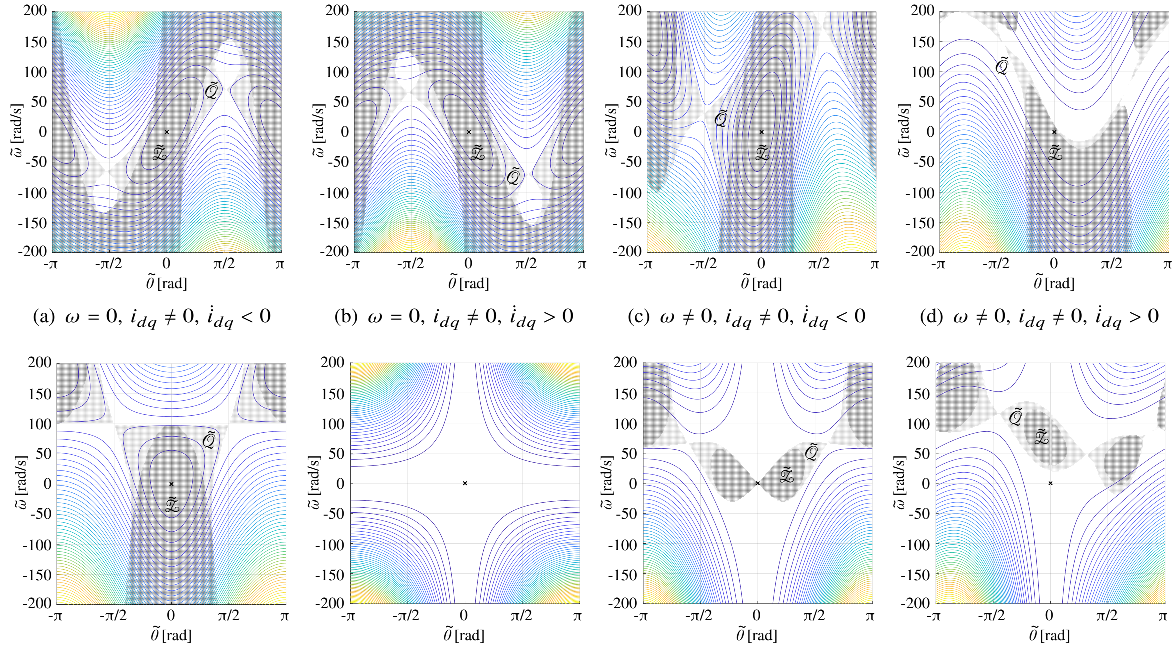

(a) $\omega = 0,\ i_{dq} \neq 0,\ \dot{i}_{dq} < 0$ (b) $\omega = 0,\ i_{dq} \neq 0,\ \dot{i}_{dq} > 0$ (c) $\omega \neq 0,\ i_{dq} \neq 0,\ \dot{i}_{dq} < 0$ (d) $\omega \neq 0,\ i_{dq} \neq 0,\ \dot{i}_{dq} > 0$

(e) $\omega \neq 0,\ i_{dq} = 0,\ \dot{i}_{dq} = 0$ (f) Bno: $\omega = 0,\ \dot{i}_{dq} = 0$ (g) Bno: $\omega \neq 0,\ \dot{i}_{dq} = 0$ (h) Bno: $\omega \neq 0,\ \dot{i}_{dq} \neq 0$

Fig. 2. Cost function $\tilde{c}([\tilde{\theta}, \tilde{\omega}]')$ sublevel sets, set of local strict convexity $\tilde{\mathscr{Z}}$, and set of local quasiconvexity $\tilde{\mathscr{Q}}$ of ipmsm ($L_\Delta = 2.4$mH, $\psi = 0.3491$Wb): typical operating ponts and bad native operation points (bno: $i_{dq} = [-\psi/(2L_\Delta), 0]'$)

where $\bar{\mathbf{P}}(2\theta) = \left[[\cos 2\theta, \sin 2\theta]', [\sin 2\theta, -\cos 2\theta]'\right]$ and $\mathbf{I}$ is the identity matrix. Hence the $\alpha\beta$ dynamic model is

$$\bar{v}_{\alpha\beta} = \left(L_\Sigma \mathbf{I} + L_\Delta \bar{\mathbf{P}}(2\theta)\right) \dot{i}_{\alpha\beta} + 2L_\Delta \omega \mathbf{J}\bar{\mathbf{P}}(2\theta) i_{\alpha\beta} + \omega\psi q(\theta), \quad (11)$$

where $\psi q(\theta) = \mathbf{J}\mathbf{P}(\theta)'\psi_r$ with $q(\theta) = [-\sin(\theta), \cos(\theta)]'$. The $\alpha\beta$ model has an explicit dependence on the position and speed. This model can be written in state-space form with state $i_{\alpha\beta}$, input $\bar{v}_{\alpha\beta}$, and unknown parameters $[\theta, \omega]'$.

IV. Position and Speed Estimation

A. Definitions and general properties

Direct position and speed estimation uses the dynamic model (11) to issue the normalized estimates $\hat{z} = [\hat{\bar{\theta}}, \hat{\bar{\omega}}]' = [\hat{\theta}/\Theta, \hat{\omega}/\Omega]'$, where $\Theta = \pi$ and $\Omega \in \mathbb{R}_{>0}$ is the rated speed. The estimates describe the parameters $z = [\bar{\theta}, \bar{\omega}] = [\theta/\Theta, \omega/\Omega]'$ with error $\tilde{z} = z - \hat{z} = [\tilde{\bar{\theta}}, \tilde{\bar{\omega}}] = [\tilde{\theta}/\Theta, \tilde{\omega}/\Omega]'$. The dynamic model (11) is written as a function of the estimates

$$\begin{aligned} r(\hat{z}) = &\left(L_\Sigma \mathbf{I} + L_\Delta \bar{\mathbf{P}}(2\hat{\theta})\right) \dot{i}_{\alpha\beta} \\ &+ 2L_\Delta \hat{\omega} \mathbf{J}\bar{\mathbf{P}}(2\hat{\theta}) i_{\alpha\beta} + \psi\hat{\omega} q(\hat{\theta}) - \bar{v}_{\alpha\beta}, \end{aligned} \quad (12)$$

where $\dot{i}_{\alpha\beta}$, $i_{\alpha\beta}$, and $\bar{v}_{\alpha\beta}$ are known at a given time instant t even in absence of a position and speed sensor. Without loss of generality, we introduce the error function, substitute $\bar{v}_{\alpha\beta}$ as they are defined by the dynamic equation (11), as well as $i_{\alpha\beta} = \mathbf{P}'(\theta) i_{dq}$ and $\dot{i}_{\alpha\beta} = \mathbf{P}'(\theta)\left(\dot{i}_{dq} + \omega \mathbf{J} i_{dq}\right)$ [8]

$$\begin{aligned} \tilde{r}(\tilde{z}) = &L_\Delta \left(\mathbf{I} - \mathbf{P}(2\tilde{\theta})\right)\left(\dot{i}_{dq} - \omega \mathbf{J} i_{dq}\right) + 2\tilde{\omega} L_\Delta \mathbf{J} i_{dq} \\ &+ \omega\psi\left(\bar{q}(2\tilde{\theta}) - \bar{q}(\tilde{\theta})\right) + \tilde{\omega}\psi\bar{q}(\tilde{\theta}), \end{aligned} \quad (13)$$

where $\bar{q}(\tilde{\theta}) = [\sin(\tilde{\theta}), \cos(\tilde{\theta})]'$.

Lemma 1. *The cost function $\tilde{c}(\cdot)$ is invariant with respect to rotor position θ and depends only on the estimation error $\tilde{\theta}$.*

Proof. Obvious since (13) depends only on $\tilde{\theta}$. □

Lemma 1 formally states that a synchronous machine responds to a position error $\tilde{\theta}$ independent of the rotor position θ due to rotational symmetry. Hence, the behavior of direct position and speed estimation can be studied for a single position, e.g. $\theta = 0$, without loss of generality. The cost function $\tilde{c}(\cdot)$ and estimation problem (4) follows immediately from $\tilde{r}(\cdot)$.

B. Local position and speed identifiability

To investigate the cost function properties, we introduce the difference flux $\xi_{dq} = 2L_\Delta i_{dq} + \psi_r$ with derivative $\dot{\xi}_{dq} = 2L_\Delta \dot{i}_{dq}$.

Theorem 1. *The origin $\tilde{c}(0)$ is strictly convex iff*

$$\omega\|\xi_{dq}\|^2 \neq \dot{\xi}_{dq}' \mathbf{J}\xi_{dq} \;\Leftrightarrow\; \xi_{dq}'\mathbf{J}(\dot{\xi}_{dq} - \omega\mathbf{J}\xi_{dq}) \neq 0.$$

Proof. We study the convexity in the origin $\tilde{z} = 0$. The Hessian is $\mathscr{H}_{\tilde{c}}(0) = [[d_1, d_2]', [d_2, d_3]']$ with

$$\begin{aligned} d_1 &= 2\Theta^2\left((\dot{\xi}_d + \omega\xi_q)^2 + (\dot{\xi}_q - \omega\xi_d)^2\right) = 2\Theta^2\|\dot{\xi}_{dq} - \omega\mathbf{J}\xi_{dq}\|^2, \\ d_2 &= 2\Theta\Omega(\dot{\xi}_d\xi_d + \dot{\xi}_q\xi_q) = 2\Theta\Omega\dot{\xi}_{dq}'\xi_{dq}, \\ d_3 &= 2\Omega^2\left(\xi_d^2 + \xi_q^2\right) = 2\Omega^2\|\xi_{dq}\|^2. \end{aligned} \quad (14)$$

Furthermore, the second order principal minor is

$$\begin{aligned} D = d_1 d_3 - d_2^2 &= 4\Theta^2\Omega^2\left(\omega\|\xi_{dq}\|^2 - \dot{\xi}_{dq}'\mathbf{J}\xi_{dq}\right)^2 \\ &= 4\Theta^2\Omega^2\left(\xi_{dq}'\mathbf{J}(\dot{\xi}_{dq} - \omega\mathbf{J}\xi_{dq})\right)^2. \end{aligned} \quad (15)$$

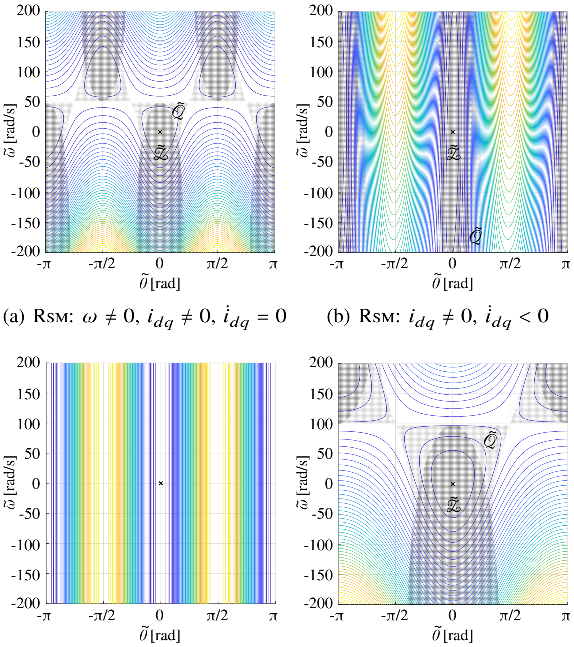

(a) Rsm: $\omega \neq 0$, $i_{dq} \neq 0$, $\dot{i}_{dq} = 0$ (b) Rsm: $i_{dq} \neq 0$, $\dot{i}_{dq} < 0$

(c) Rsm bno (d) Spmsm: $\omega \neq 0$

Fig. 3. Cost function $\tilde{c}([\tilde{\theta}, \tilde{\omega}]')$ sublevel sets, set of local strict convexity $\tilde{\mathscr{Z}}$, and set of local quasiconvexity $\tilde{\mathscr{Q}}$ of rsm ($L_\Delta = 2.4$mH, $\psi = 0$Wb) and spmsm ($L_\Delta = 0$mH, $\psi = 0.3491$Wb): typical operating ponts and bad native operation points (bno: $i_{dq} = [-\psi/(2L_\Delta), 0]'$)

Since all principle minors (d_1, d_3, D) are nonnegative, $\tilde{c}(0)$ is convex [10]. In addition, the function is strictly convex, when the leading principle minors are positive definite. This holds when $D > 0$ since $D > 0$ implies $d_1 > 0$ and $d_3 > 0$. □

The Theorem 1 shows that θ and ω are locally identifiable unless the machine is operated in specific operation points, named *bad native operation points* (bno). The parameters are identifiable in machines with a salience $L_\Delta \neq 0$ and suitable perturbation $\dot{i}_{dq}$, unless $i_{dq} = [-\psi/(2L_\Delta), 0]'$. This bno does not exist for spmsm and is of limited relevance for ipmsm, where it is located on the opposite half-plane of the mtpa trajectory [9]. Examples are shown in Fig. 2(f), Fig. 2(g), and Fig. 2(h). For rsm, the bno is $i_{dq} = 0$ and needs to be avoided at any speed (and perturbation). For spmsm, the bno is $\omega = 0$.

C. Steady-state local identifiability and perturbation strategies

Motor drive systems tend to work in close to steady-state conditions ($\dot{i}_{dq} = 0$) in many applications since the electrical transients tend to be fast compared to the mechanical ones.

Corollary 1. *Steady-state ($\dot{i}_{dq} = 0$) local identifiability holds iff $\omega \neq 0$ and $2L_\Delta i_{dq} + \psi_r \neq 0$.*

Proof. Theorem 1 requires $\omega\|\xi_{dq}\|^2 \neq 0$ at $\dot{\xi}_{dq} = \dot{i}_{dq} = 0$. □

Hence, θ (and ω) cannot be estimated at $\omega = 0$ in steady-state conditions in any machine. Hence, low speed estimation requires a perturbation of the states, i.e. currents. In general, any strategy is valid that adds a (high-frequency) zero-mean perturbation (with $\dot{i}_{dq} \neq 0$) to a (steady-state) operation point i_{dq}.

Periodic perturbation is typically used in combination with pwm inverters using vector control [1] or ccs-mpc [8]. A well defined periodic signal is added to a given steady state operation point [1]. Typical approaches are the injection of a pulsating sinusoidal signal along a predefined dq [1], [11], [12] or zero [13] axis or a vector that rotates at high-frequency in the dq space [11], [12]. Since the perturbation is needed only at low speed, the injection magnitude can be reduced as the speed increases.

Random perturbation exploits switching harmonics in the motor currents and is typically used in motor control methods that apply switching states directly, e.g. direct torque control (dtc) [14], [15] or fcs-mpc [2], [16], [17]. The lack of pwm makes the injection and reconstruction of a well defined high-frequency signal challenging. Hence, it is beneficial to rely on the current ripple that is fully visible in the measurements of such methods [2], [8].

V. Numerical Computation of Estimates

At each sampling instant, a numerical solver obtains the stationary point of the cost function $\bar{c}(\cdot)$ by producing a sequence of iterates $\hat{z}_0, \ldots, \hat{z}_j, \ldots, \hat{z}^\star$. The sequence starts with an initial guess $\hat{z}_g = \hat{z}_0$ and ends with the optimizer $\hat{z}^\star$ that identifies the (normalized) parameters z with accuracy, i.e. $\|z - \hat{z}^\star\| \leq \epsilon$, $\epsilon \in \mathbb{R}_{>0}$. The sequence is generated identifying a suitable step Δ_j and stepsize α_j

$$\hat{z}_{j+1} = \hat{z}_j + \alpha_j \Delta_j. \tag{16}$$

The stepsize α_j is typically chosen with a suitable linesearch technique to accelerate and robustify convergence [18]. As any linesearch technique is applicable, golden section search [18] is used throughout this research. The step Δ_j can be determined with first or second order methods.

The *nonlinear conjugate gradient* method is a first order method that identifies a stationary point of a differentiable cost function. It avoids the "zig-zag" nature of the steepest descent method by following the conjugate direction $\Delta_j = -\nabla c(\hat{z}_j) + \beta_j \Delta_{j-1}$ (with $\Delta_0 = -\nabla c(\hat{z}_j)$). The parameter β_j can be computed using several formulae [18] and we use the Fletcher-Reeves formula $\beta_j = \|\nabla c(\hat{z}_j)\|^2 / \|\nabla c(\hat{z}_{j-1})\|^2$. The conjugate gradient method is observed to identify estimates robustly even if the cost is quasi-convex. The second order *Newton* method identifies the roots of a twice differentiable function by approximating the function with its second order Taylor series in $\hat{z}_j$. This approximation can be solved for its minimum resulting in $\Delta_j = -\mathscr{H}_{\tilde{c}}^{-1}(\hat{z}_j)\nabla c(\hat{z}_j)$ [18].

A reference solver is implemented that combines the benefits of the gradient and Newton method. Since $\nabla c(\hat{z}_j)$ and $\mathscr{H}_{\tilde{c}}(\hat{z}_j)$ are computed at each time step, the solver can check efficiently for strict convexity and quasi-convexity [7] resulting in the step

$$\Delta_j = \begin{cases} -\mathscr{H}_{\tilde{c}}^{-1}(\hat{z}_j)\nabla c(\hat{z}_j), & \text{if } \hat{z}_j \in \mathscr{Z} \\ -\nabla c(\hat{z}_j) + \beta_j \Delta_{j-1}, & \text{if } \hat{z}_j \in \mathscr{Q} \setminus \mathscr{Z} \text{ and } j > 0 \\ -\nabla c(\hat{z}_j), & \text{if } \hat{z}_j \in \mathscr{Q} \setminus \mathscr{Z} \text{ and } j = 0 \\ 0. & \text{otherwise.} \end{cases} \tag{17}$$

If $\hat{z}_j$ is in the strictly convex region, the Newton step can be employed to maximize convergence. If $\hat{z}_j$ is in the quasi-convex

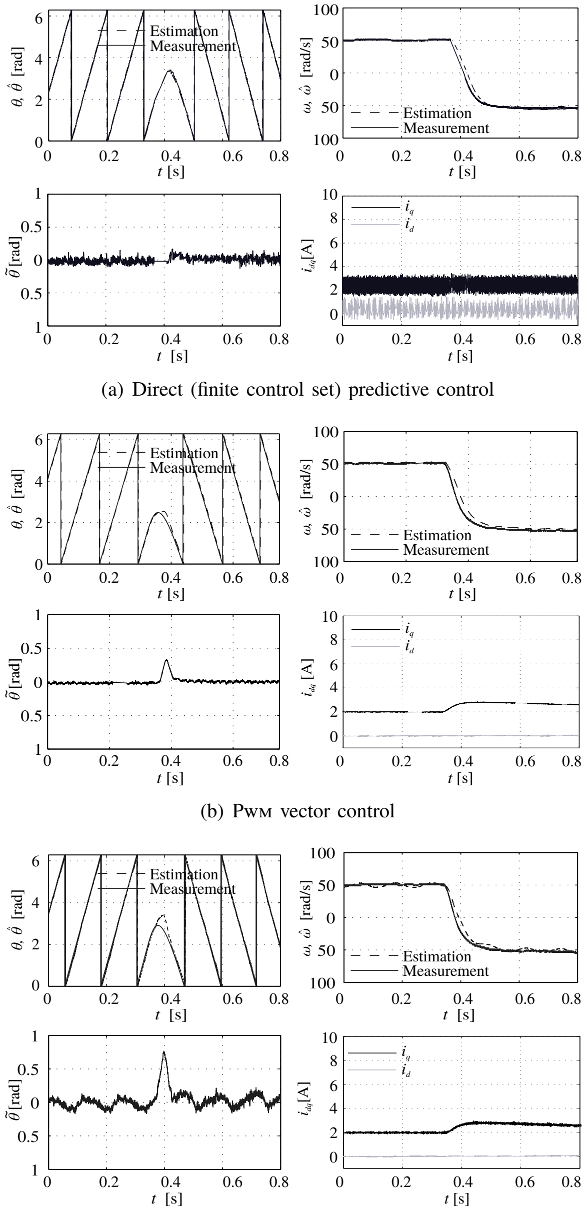

(a) Direct (finite control set) predictive control

(b) Pwm vector control

(c) Pwm vector control with disturbance (5% of rated voltage)

Fig. 4. Experimental zero-speed crossing with direct position and speed sensorless: position measurement θ and estimate $\hat{\theta}$, position error $\tilde{\theta}$, speed measurement ω and estimate $\hat{\omega}$, d and q currents i_{dq}

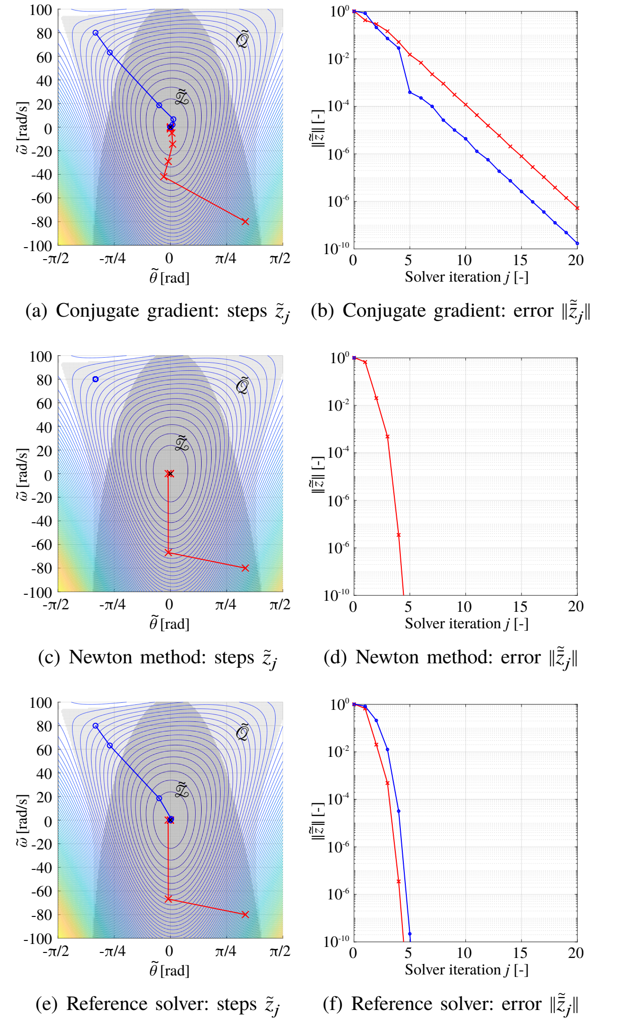

(a) Conjugate gradient: steps $\tilde{z}_j$ (b) Conjugate gradient: error $\|\tilde{z}_j\|$

(c) Newton method: steps $\tilde{z}_j$ (d) Newton method: error $\|\tilde{z}_j\|$

(e) Reference solver: steps $\tilde{z}_j$ (f) Reference solver: error $\|\tilde{z}_j\|$

Fig. 5. Numerical solver performance: the conjugate gradient method converges for any initial guess $\tilde{z}_g \in \tilde{\mathcal{Q}}$ (circles), the Newton method converges with fast rate for any initial guess $\tilde{z}_g \in \tilde{\mathcal{Z}}$ (crosses), the reference solver uses the conjugate gradient step for any $\tilde{z}_j \in \tilde{\mathcal{Q}} \setminus \tilde{\mathcal{Z}}$ and Newton step for any $\tilde{z}_j \in \tilde{\mathcal{Z}}$.

region, the conjugate gradient step is used to increase the region of convergence. If the problem lacks quasi-convexity, the solver cannot issue a meaningful estimate. Instead, the guess $\hat{z}_g$ is returned, which corresponds to the extrapolated estimate from the previous sample. The performance of the algorithm is shown in Fig. 5 and Fig. 6.

VI. Results

The drawings and test-bench results in this paper are obtained on a ipmsm machine with rated speed $n_r = 1800$rpm, rated torque $T_r = 29.7$Nm, 5 pole pairs, rated line to line voltage $V_{r,ll} = 460\text{V}_{\text{rms}}$, rated current $I_r = 9.4\text{A}_{\text{rms}}$, and electric parameters $L_d = 10.5$mH, $L_q = 12.9$mH, $\psi = 349.1$mWb, and $R = 0.4\Omega$. The spmsm and rsm drawings are obtained by setting $L_d = L_q$ and $\psi = 0$mWb, respectively. The machine is fed by a SiC inverter with dc-bus voltage $V_c = 800$V, sampling period $T_s = 100\mu$s, and interlock times $T_i = 0.3\mu$s. The switching frequency is $1/T_s$ in pwm vector control and 2-3kHz in fcm-mpc. The stator resistance and interlock times are compensated using $\bar{v}_{\alpha\beta}$. The control platform is a 200MHz TI C2000 Delfino microcontroller.

A. Test bench results

The operation of direct position and speed sensorless estimation is shown on a *test bench* and the results are reported in Fig. 4. The motor drive performs a position sensorless zero crossing at ±50rpm. Fig. 4(a) shows θ and ω estimation with fcm-mpc that performs the zero crossing exploiting the perturbation provided by the switching ripple. Fig. 4(b) shows θ and ω estimation with pwm vector control that introduces a zero-mean perturbation at $|\omega| < 50$rpm. Fig. 4(c) shows θ and ω estimation with pwm

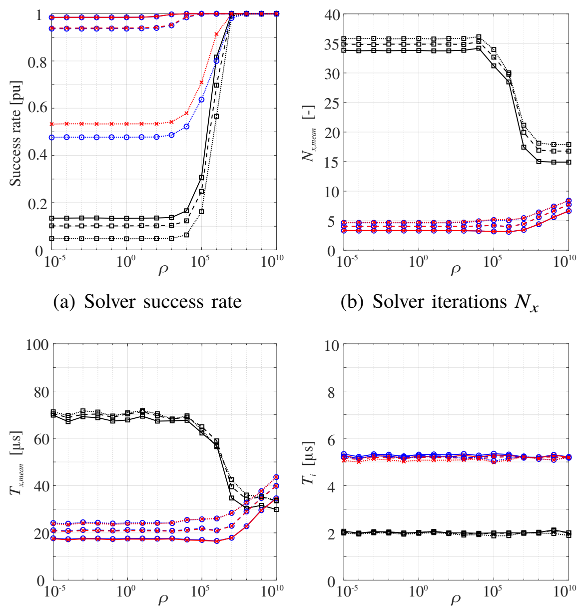

(a) Solver success rate (b) Solver iterations N_x

(c) Solver exec. time T_x (d) Exec. time per iteration T_i

Fig. 6. Performance of numerical solvers (1M random operation points per marker) with random perturbation and robust perturbation ($\dot{\xi}_{dq} = \gamma \mathbf{J} \xi_{dq}$) for normalized initial guesses $\tilde{\tilde{z}}_g = [\tilde{\theta}_g/\Theta, \tilde{\omega}_g/\Omega]'$ satisfy $\|\tilde{\tilde{z}}_g\| \leq 1\%$ (solid lines), $\|\tilde{\tilde{z}}_g\| \leq 10\%$ (dashed lines), and $\|\tilde{\tilde{z}}_g\| \leq 100\%$ (dotted lines) as function of the convexification parameter ρ: reference solver (crosses, red), Newton solver (circles, blue), and conjugate gradient solver (squares, black)

vector control in presence of a disturbance $\|w\| = 5\%\mathrm{V}_r$. Additonal test-bench results of direct θ and ω estimation (with output PLL filtering) are available in literature for PWM control [1], FCM-MPC [2], and induction machine [4].

B. Numerical solver convergence and performance

Real-time capable solvers are investigated and typical behavior is reported in Fig. 5. In Fig. 5(a) and Fig. 5(b), the conjugate gradient method is shown to converge for any $z_g \in \mathcal{Q}$. In Fig. 5(c) and Fig. 5(d), the Newton method is shown to converge at a much faster rate for $z_g \in \mathcal{Z}$, except for $z_g \in \mathcal{Q} \setminus \mathcal{Z}$. The reference solver uses the Newton method for $z_j \in \mathcal{Z}$ for performance and the conjugate gradient method for $z_j \in \mathcal{Q} \setminus \mathcal{Z}$ to expand the feasible initial guesses (Fig. 5(e) and Fig. 5(f)).

The real-time performance of the solvers is shown in Fig. 6, where each marker corresponds to 1 million random operation points (θ, ω, $i_{\alpha\beta}$, and $\dot{i}_{\alpha\beta}$) and the normalized initial guesses satisfy $\|\tilde{\tilde{z}}_g\| \leq 1\%$ (solid lines), $\|\tilde{\tilde{z}}_g\| \leq 10\%$ (dashed lines), and $\|\tilde{\tilde{z}}_g\| \leq 100\%$ (dotted lines). The results are plotted as function of the convexification factor ρ. Fig. 6(a) show the success rate such that z can be identified. As expected, the success rate increases significantly at high ρ as the cost function becomes essentially convex. The reference solver (and Newton method) achieve a success rate exceeding 98.5% and 93.5% for 1% and 10% initial errors, respectively (these results include low speed cases without perturbation).

The execution time is approximately 5µs for one Newton step and 2µs for one conjugate gradient step per iteration. For $\rho < 10^5$, the reference solver (and Newton method) require 3 to 5 iterations N_x to converge resulting in 15µs to 25µs total execution time T_x. In practice, the solver iterations can be limited to a maximum value to guarantee a maximum execution time.

VII. Conclusion

This paper develops the local identifiability theory such that direct estimation can obtain parameters instantaneously, i.e. within one sampling period. We show that parameters can be uniquely identified if the cost function formulation is strictly convex at the parameter value and an initial guess lies in its quasiconvex neighborhood. The formulation is shown to be robust in the sense that a bounded disturbance results in a bounded estimation error if the cost function is strictly convex in a neighborhood of the estimate. The concept is applied to position and speed estimation in synchronous motor drives, where 3-5 solver iterations are sufficient to identify the parameters with high precision (10^{-4} error), and operation is feasible with a single solver iteration. We demonstrate that the parameters can be identified in more than 98.5% of all possible operation points "instantaneously", i.e. with the measurements of one sampling instant, based on a reasonable initial guess (position and speed are not globally observable). In the remaining cases, an estimates can be issued through extrapolation.

VIII. Acknowledgement

The author thanks Dr. Shamsuddeen Nalakath for his support in obtaining the test-bench results.

References

[1] Y. Sun *et al.*, "Unified wide speed range ipm sensorless scheme using nonlinear optimization," *IEEE Trans. Power Electron.*, vol. 32, pp. 6308–6322, 2017.

[2] S. Nalakath *et al.*, "Optimization-based position sensorless finite control set model predictive control for ipmsms," *IEEE Trans. Power Electron.*, vol. 33, pp. 8672–8682, 2018.

[3] X. Yong and M. Preindl, "Optimization-based position estimation of pm synchronous machine motor drives with magnetic saturation," in *IEEE SLED*, 2018.

[4] A. D. Callegaro *et al.*, "Optimization-based position sensorless for induction machines," in *IEEE ITEC*, 2018.

[5] S. Ibarra-Rojas *et al.*, "Global observability analysis of sensorless induction motors," *Automatica*, vol. 40, pp. 1079–1085, 2004.

[6] A. Tilli and C. Conficoni, "Semiglobal uniform asymptotic stability of an easy-to-implement pll-like sensorless observer for induction motors," *IEEE Trans. Autom. Control*, vol. 61, pp. 3612–3618, 2016.

[7] G. Giorgi *et al.*, *Mathematics of Optimization: Smooth and Nonsmooth Case*. Elsevier Science, 2004.

[8] M. Preindl, "Robust control invariant sets and lyapunov-based mpc for ipm synchronous motor drives," *IEEE Trans. Ind. Electron.*, vol. 63, pp. 3925–3933, 2016.

[9] M. Preindl and S. Bolognani, "Optimal state reference computation with constrained MTPA criterion for PM motor drives," *IEEE Trans. Power Electron.*, vol. 30, pp. 4524–4535, 2015.

[10] G. T. Gilbert, "Positive definite matrices and sylvester's criterion," *The American Mathematical Monthly*, vol. 98, pp. 44–46, 1991.

[11] N. Bianchi *et al.*, "Comparison of pm motor structures and sensorless control techniques for zero-speed rotor position detection," *IEEE Trans. Power Electron.*, vol. 22, pp. 2466–2475, 2007.

[12] D. Raca *et al.*, "Carrier-signal selection for sensorless control of PMSM at zero and very low speeds," *IEEE Trans. Ind. Appl.*, vol. 46, pp. 167–178, 2010.

[13] R. Leidhold, "Position sensorless control of PMSM based on zero-sequence carrier injection," *IEEE Trans. Ind. Electron.*, vol. 58, pp. 5371–5379, 2011.

[14] I. Takahashi and T. Noguchi, "A new quick-response and high-efficiency control strategy of an induction motor," *IEEE Trans. Ind. Appl.*, vol. IA-22, pp. 820–827, 1986.

[15] M. Depenbrock, "Direct self-control of inverter-fed induction machine," *IEEE Trans. Power Electron.*, vol. 3, pp. 420–429, 1988.

[16] M. Preindl and S. Bolognani, "Model predictive direct torque control with finite control set for PMSM drive systems, part 1: Maximum torque per ampere operation," *IEEE Trans. Ind. Inf.*, vol. 9, pp. 1912–1921, 2013.

[17] M. Preindl and E. Schaltz, "Sensorless model predictive direct current control using novel second-order PLL observer for PMSM drive systems," *IEEE Trans. Ind. Electron.*, vol. 58, pp. 4087–4095, 2011.

[18] D. Luenberger and Y. Ye, *Linear and Nonlinear Programming*. Springer, 2008.